

# Local Structure and Strain-Induced Distortion in $\text{Ce}_{0.8}\text{Gd}_{0.2}\text{O}_{1.9}$

By Anna Kossoy, Anatoly I. Frenkel,\* Qi Wang, Ellen Wachtel, and Igor Lubomirsky\*

Cerium oxide, in both pure and doped forms, is one of the most important and extensively studied oxygen ion conductors. It exhibits a number of interesting properties including ionic conductivity due to the high mobility of oxygen vacancies, a series of different phases formed upon reduction,<sup>[1]</sup> dependence of the lattice parameter and electrical properties on grain size,<sup>[2]</sup> and non-linear elastic effects, which have been named “chemical stress”<sup>[3]</sup> and “chemical strain”.<sup>[4–6]</sup> Recent structural studies, both theoretical<sup>[7]</sup> and experimental,<sup>[8–10]</sup> have been aimed at understanding the mechanism of interaction between the cations and the oxygen vacancies. These interactions are thought to be directly responsible for a number of effects such as resistance to radiation damage,<sup>[11]</sup> vacancy ordering leading to phase transformations,<sup>[1,12,13]</sup> dependence of ionic conductivity on the ionic radius of the dopant,<sup>[14]</sup> and the non-linear elastic effects. Furthermore, in addition to the fluorites, cation-vacancy interactions are observed in a number of other solids with a large concentration of oxygen vacancies, for instance, perovskites.<sup>[15]</sup> Therefore, characterizing the details of cation-vacancy interactions in  $\text{Ce}_{0.8}\text{Gd}_{0.2}\text{O}_{1.9}$  may have implications for a wider range of materials.

One property in which the cation-vacancy interaction is thought to be directly implicated is the chemical strain effect, which is the ability of thin films of  $\text{Ce}_{0.8}\text{Gd}_{0.2}\text{O}_{1.9}$  to exhibit two different elastic moduli at temperatures below 200 °C.<sup>[5,6]</sup> This effect is accompanied by an absolute change in volume of ~0.2% even when the external stress is homogeneous, which distinguishes it from the Gorsky, Snoek<sup>[16]</sup> or Zener<sup>[17]</sup> effects. The chemical strain effect has been tentatively attributed to a change in specific volume due to the interaction of the  $\text{Gd}^{3+}$  ions with oxygen vacancies (5% of all oxygen sites in  $\text{Ce}_{0.8}\text{Gd}_{0.2}\text{O}_{1.9}$ <sup>[4,5,18]</sup>). However, no evidence has been presented that the rearrangement of vacancies in  $\text{Ce}_{0.8}\text{Gd}_{0.2}\text{O}_{1.9}$  can be stress-induced, or even takes place at all. The present study uses extended X-ray absorption

fine-structure (EXAFS) spectroscopy to evaluate the local structure of strain-free nanocrystalline films of  $\text{Ce}_{0.8}\text{Gd}_{0.2}\text{O}_{1.9}$  and to compare it with that of  $\text{Ce}_{0.8}\text{Gd}_{0.2}\text{O}_{1.9}$  films with in-plane compressive strain of  $0.3\% \pm 0.1\%$ . Since the lattice parameter of  $\text{Ce}_{0.8}\text{Gd}_{0.2}\text{O}_{1.9}$  varies by a few tenths of a percent, depending on the preparation route and sample history,<sup>[6]</sup> the X-ray diffraction (XRD) and EXAFS measurements were performed on the same samples, thus permitting direct comparison of the local ion arrangement with the long-range structure. We report that even in strain-free  $\text{Ce}_{0.8}\text{Gd}_{0.2}\text{O}_{1.9}$ , interaction of oxygen vacancies with  $\text{Ce}^{4+}$  ion neighbors is favored, rather than interaction with  $\text{Gd}^{3+}$  ion neighbors. As a result,  $\text{Ce}^{4+}$  ions are shifted away from the oxygen vacancies. Furthermore, compressive strain of  $0.3\% \pm 0.1\%$  causes the Ce–O bond to contract by  $1.0\% \pm 0.5\%$ , whereas other bonds remain much less affected. This anomalous Ce–O bond contraction potentially offers a microscopic explanation for the chemical strain effect observed in  $\text{Ce}_{0.8}\text{Gd}_{0.2}\text{O}_{1.9}$ .

Films of  $\text{Ce}_{0.8}\text{Gd}_{0.2}\text{O}_{1.9}$  (200–450 nm) were deposited on a (001) Si substrate by RF sputtering and then annealed as described in refs. <sup>[4,5]</sup>. The films were kept at room temperature for > 4 months to achieve a constant value of the lattice parameter, indicating that the low-temperature equilibrium of the point defects had been reached.<sup>[6]</sup> After annealing, the in-plane stress in the  $\text{Ce}_{0.8}\text{Gd}_{0.2}\text{O}_{1.9}$  films was found to be less than 30 MPa.<sup>[4,5]</sup> The sputtering conditions were adjusted so that the annealed films comprised two groups: (1) those films that were strain free after annealing and (2) those that had a residual compressive strain of  $0.3\% \pm 0.1\%$ . The presence of strain was evident from the anisotropy of the d-spacings as measured by XRD in the iso-inclination mode.<sup>[6]</sup> According to XRD data, acquired in the  $\theta$ – $2\theta$  mode (with  $\theta$  offset of 3° for thin films in order to suppress Si single-crystal reflections from substrate), all films and the reference  $\text{CeO}_2$  and  $\text{Ce}_{0.8}\text{Gd}_{0.2}\text{O}_{1.9}$  powders were in a single fluorite phase (Fig. 2 in this work and Fig. 2 in Ref. [6]). The lattice parameters of the powders (milled parts of the sputtering targets, grain size > 1  $\mu\text{m}$ ) determined from high-angle ( $2\theta > 80^\circ$ ) measurements<sup>[19]</sup> were 5.411 Å and 5.425 Å for  $\text{CeO}_2$  and  $\text{Ce}_{0.8}\text{Gd}_{0.2}\text{O}_{1.9}$ , respectively.<sup>[6,20]</sup>

The EXAFS spectra of the  $L_{\text{III}}$  edges of Ce and Gd were collected on beam lines X18B and X19A of the National Synchrotron Light Source at Brookhaven National Laboratory (Fig. 1). To decrease correlations among the variables in the fit to the  $\text{Ce}_{0.8}\text{Gd}_{0.2}\text{O}_{1.9}$  EXAFS data, we performed multiple edge analysis by fitting the Gd and Ce edge data simultaneously. Therefore, the EXAFS results could be obtained more reliably not only for the 1NN (cation–oxygen) pairs, but also for the 2NN

[\*] Prof. I. Lubomirsky, A. Kossoy  
Department of Materials & Interfaces, Weizmann Institute of Science  
Rehovot 76100 (Israel)  
E-mail: Igor.Lubomirsky@weizmann.ac.il  
Prof. A. I. Frenkel, Dr. Q. Wang  
Department of Physics, Yeshiva University  
New York, NY 10016 (USA)  
E-mail: anatoly.frenkel@yu.edu  
Dr. E. Wachtel  
Chemical Research Support, Weizmann Institute of Science  
Rehovot 76100 (Israel)

DOI: 10.1002/adma.200902041

(cation–cation) pairs. Best fit values of structural parameters obtained by EXAFS analysis are reported together with their uncertainties defined as the 95% confidence limits. Standard CeO<sub>2</sub> and Ce<sub>0.8</sub>Gd<sub>0.2</sub>O<sub>1.9</sub> powders were used to verify the fitting with the IFEFFIT data analysis package and the EXAFS-derived bond lengths in the strain-free films of Ce<sub>0.8</sub>Gd<sub>0.2</sub>O<sub>1.9</sub> were

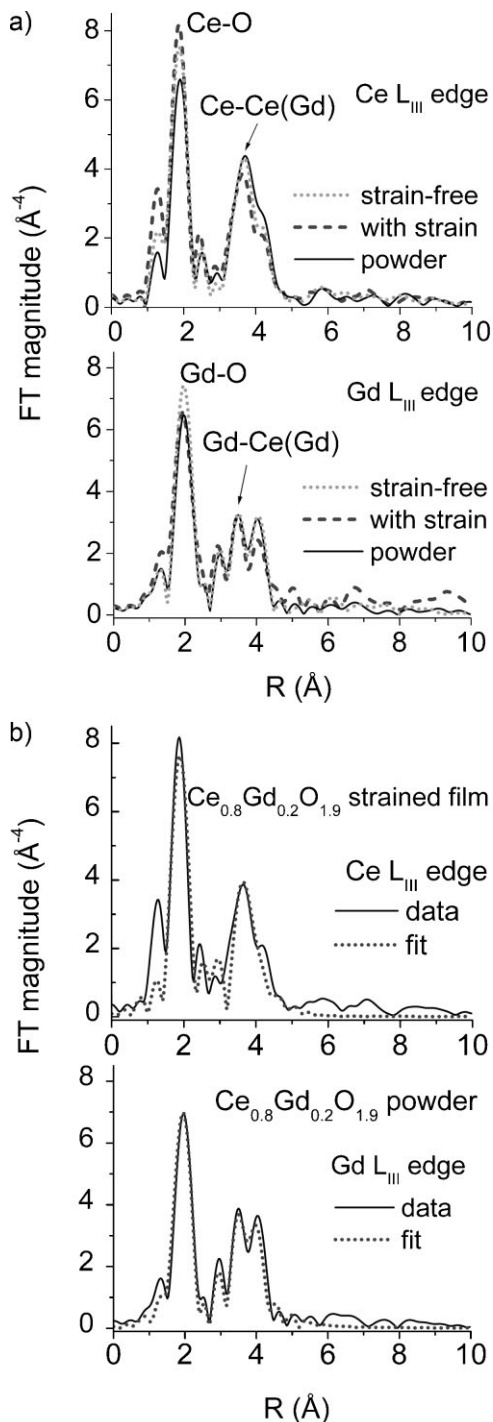


**Figure 1.** Fourier transform magnitudes of the L<sub>III</sub> edge EXAFS spectra of Ce and Gd for a) powders and thin films of Ce<sub>0.8</sub>Gd<sub>0.2</sub>O<sub>1.9</sub> with and without strain, and b) data and FEFF6 fits.

measured to be the same as in the powders, within the uncertainties (Table 1, Fig. 2). Further experimental details concerning the EXAFS data acquisition and fitting are given in the Supporting Information.

For strain-free films, the length of the Gd–O bond,  $L_{Gd-O} = 2.375 \pm 0.016 \text{ \AA}$ , is greater than the length of the Ce–O bond,  $L_{Ce-O} = (2.325 \pm 0.007) \text{ \AA}$ , which is consistent with the difference in the ionic radii between Gd<sup>3+</sup> ( $r_{Gd^{3+}} = 1.19 \text{ \AA}$ ) and Ce<sup>4+</sup> ( $r_{Ce^{4+}} = 1.11 \text{ \AA}$ ).<sup>[21]</sup> However, the XRD-derived bond length  $L_{Cation-O}^{XRD} = (2.349 \pm 0.002) \text{ \AA}$  is much larger than the weighted average:

$$L_{Cation-O} = 0.2L_{Gd-O} + 0.8L_{Ce-O} = (2.335 \pm 0.007) \text{ \AA} \quad (1)$$

although one would expect that for a single-phase material the weighted average of the 1NN bond lengths would be close to the XRD-derived values.<sup>[22,23]</sup> The observed difference may be attributed to the presence of 5% oxygen vacancies, which do not contribute to the EXAFS-derived cation–oxygen distances but affect the XRD-derived average 1NN distance. Thus the average cation–vacancy distance can be estimated as:

$$\begin{aligned} \overline{L_{Cation-vacancy}} &= (L_{Cation-O}^{XRD} - 0.95L_{Cation-O})/0.05 \\ &= (2.615 \pm 0.14) \text{ \AA} \end{aligned} \quad (2)$$

Equation (2) implies that either one or both cations shift away from the vacancy by  $\Delta L = \overline{L_{Cation-vacancy}} - L_{Cation-O}^{XRD} = 2.615 \text{ \AA} - 2.355 \text{ \AA} = (0.27 \pm 0.16) \text{ \AA}$ . However, because the average structure of the material remains that of the fluorite phase, one must conclude that the shifts of the individual cations do not display long range correlations and only local deviations from the average fluorite structure are present.

The EXAFS-derived Gd–Ce distance for powders,  $L_{Gd-Ce} = (3.811 + 0.015) \text{ \AA}$ , is considerably shorter than the Ce–Ce distance ( $L_{Ce-Ce} = (3.846 + 0.008) \text{ \AA}$ ) for powders and strain-free films (a total of five samples studied). Using the EXAFS-derived value for  $L_{Gd-Gd}$  in Ref. [9],  $(3.91 \pm 0.1) \text{ \AA}$ , one can see that the concentration-weighted average value of the

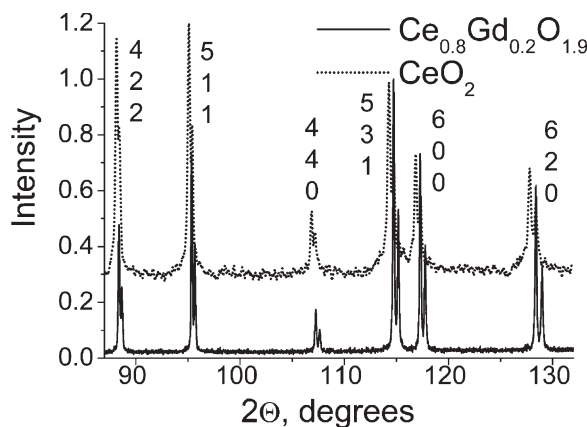


**Figure 2.** High-angle diffraction patterns of target powders. Both samples are consistent with a single-phase fluorite structure. Peak splitting is due to the presence of Cu K $\alpha$ 2. The Miller indices are shown.

**Table 1.** Inter-atomic distances and mean square relative displacements ( $\sigma^2$ ) derived from EXAFS analysis of  $\text{Ce}_{0.8}\text{Gd}_{0.2}\text{O}_{1.9}$  powder and thin films.

Bond type		XRD ( $a = 5.425 \text{ \AA}$ )	Powder	Annealed film without strain	Annealed film with strain
Gd–O	$R$ ( $\text{\AA}$ )	2.349	$2.375 \pm 0.016$	$2.375 \pm 0.008$	$2.365 \pm 0.015$
	$\sigma^2$ ( $\text{\AA}^2$ )		$0.007 \pm 0.002$	$0.006 \pm 0.001$	$0.007 \pm 0.002$
Ce–O	$R$ ( $\text{\AA}$ )	2.349	$2.319 \pm 0.007$	$2.325 \pm 0.008$	$2.302 \pm 0.007$
	$\sigma^2$ ( $\text{\AA}^2$ )		$0.003 \pm 0.001$	$0.002 \pm 0.001$	$0.001 \pm 0.001$
Gd–Ce/Ce–Gd	$R$ ( $\text{\AA}$ )	3.836	$3.811 \pm 0.015$	$3.818 \pm 0.009$	$3.788 \pm 0.017$
	$\sigma^2$ ( $\text{\AA}^2$ )		$0.008 \pm 0.002$	$0.010 \pm 0.001$	$0.010 \pm 0.002$
Ce–Ce	$R$ ( $\text{\AA}$ )	3.836	$3.846 \pm 0.008$	$3.844 \pm 0.008$	$3.829 \pm 0.010$
	$\sigma^2$ ( $\text{\AA}^2$ )		$0.004 \pm 0.001$	$0.003 \pm 0.001$	$0.004 \pm 0.001$

cation–cation bonds matches the XRD value ( $(3.836 \pm 0.002) \text{ \AA}$ ):

$$L_{\text{Cation-Cation}} = (0.8)^2 \cdot L_{\text{Ce-Ce}} + 2 \cdot 0.8 \cdot 0.2 \cdot L_{\text{Gd-Ce}} + (0.2)^2 L_{\text{Gd-Gd}} = 3.837 \text{ \AA} \quad (3)$$

The large derived cation–vacancy distance (Eq. 2) and the fact that  $L_{\text{Gd-Ce}} < L_{\text{Ce-Ce}}$  while  $L_{\text{Ce-O}} < L_{\text{Gd-O}}$ , taken together, indicate that the probability of finding a vacancy in the vicinity of a Gd ion is less than that for a Ce ion. This conclusion is supported by theoretical calculations: the defect association energy disfavors interaction of large dopants with oxygen vacancies.<sup>[7]</sup> Therefore, in the case of  $\text{Ce}_{0.8}\text{Gd}_{0.2}\text{O}_{1.9}$ ,  $\text{Ce}^{4+}$ –oxygen vacancy interaction is favored. Similar relations among the bond lengths for Ce–Gd–O and Ce–Y–O powders were obtained by Deguchi et al. using K-edge EXAFS analysis.<sup>[8]</sup> The conclusion that there is a strong interaction between vacancies and cations is also consistent with the fact that solid solutions  $\text{Ce}_{1-x}\text{Gd}_x\text{O}_{2-x/2}$  ( $0 < x < 0.4$ ) with nominally fluorite structure exhibit a strong deviation from Vegard's law<sup>[9]</sup> (Fig. 1 in Ref. [6]).

The mean EXAFS-derived Ce–O inter-atomic distance in the films with compressive strain of  $0.3\% \pm 0.1\%$  is smaller by  $1\% \pm 0.5\%$  than the mean distance in the strain-free films (Table 1, Fig. 3) and the difference is statistically significant. On the other hand, the Gd–O, Gd–Ce, and Ce–Ce distances show either non-significant or marginally significant contraction with respect to the powder or strain-free film (Fig. 3). Therefore, while the Gd–O environment is stable in the presence of macroscopic strain, the Ce ion shifts further away from the vacancy towards its oxygen neighbors by more than would be expected from the magnitude of the strain. This difference in behavior of the Gd–O and the Ce–O bonds under strain is consistent with the conclusion that the oxygen vacancies prefer the  $\text{Ce}^{4+}$  environment. We suggest that this finding offers a microscopic explanation for the elastic anomalies, i.e., chemical strain effect, observed in  $\text{Ce}_{0.8}\text{Gd}_{0.2}\text{O}_{1.9}$ . The additional shift of  $\text{Ce}^{4+}$  ions away from the vacancies is an efficient strain-relieving mechanism and may be the most probable cause for the net change in volume ( $>0.2\%$ ) observed under strain.<sup>[5]</sup> One should note that the chemical strain effect in  $\text{Ce}_{0.8}\text{Gd}_{0.2}\text{O}_{1.9}$  vanishes above  $250 \text{ }^\circ\text{C}$ <sup>[6]</sup> where the mobility of the vacancies is still very low. Therefore, although strain-induced reorientation of a  $\text{Ce}^{4+}$ –vacancy pair, similar to the Zener effect (stress-induced reorientation of asymmetric defects),<sup>[17]</sup> is possible, it is not expected to contribute significantly to the stress-relaxation in  $\text{Ce}_{0.8}\text{Gd}_{0.2}\text{O}_{1.9}$ .

Three conclusions may be drawn from our findings. First, in  $\text{Ce}_{0.8}\text{Gd}_{0.2}\text{O}_{1.9}$  at room temperature, interaction of oxygen vacancies with  $\text{Ce}^{4+}$  ion neighbors is favored, rather than interaction with  $\text{Gd}^{3+}$  ion neighbors. The Ce–vacancy distance is larger than predicted by the XRD-determined fluorite structure. Most probably, this is also true for other aliovalent-doped ceria where the dopants are larger than the host cation. Second, the observed anomalous change in the local environment of  $\text{Ce}^{4+}$  under compressive strain is a probable cause of the deviation from linear elasticity in  $\text{Ce}_{0.8}\text{Gd}_{0.2}\text{O}_{1.9}$ .<sup>[5,6]</sup> One would expect that other pure and doped ceria compounds containing a large concentration of vacancies will also exhibit elastic anomalies if the dopant ion is larger than  $\text{Ce}^{4+}$ , including the case of oxygen deficient ceria,

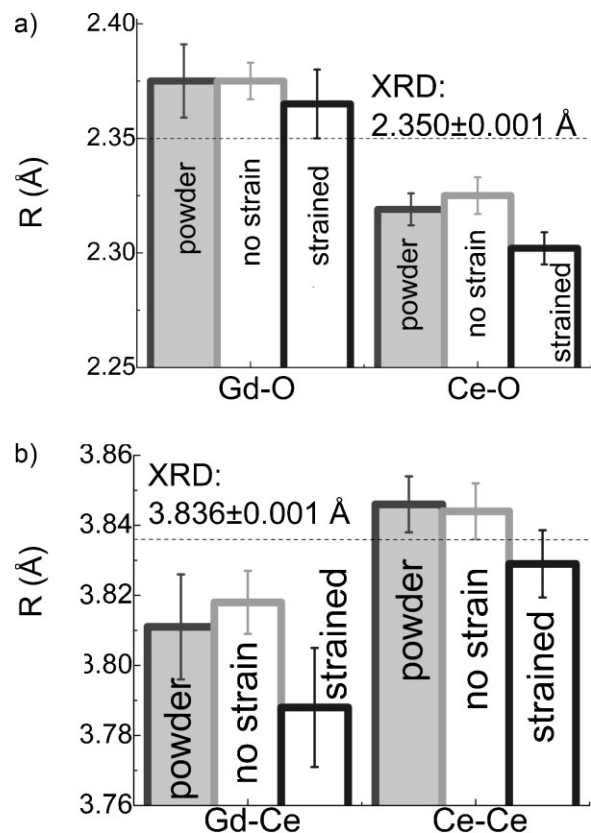


**Figure 3.** EXAFS-derived bond lengths for a) cation–anion and b) cation–cation pairs obtained for the coarse-grain powders and thin films of  $\text{Ce}_{0.8}\text{Gd}_{0.2}\text{O}_{1.9}$  with and without compressive strain (data taken from Table 1).

$\text{CeO}_{2-x}$ .  $\text{Ce}^{3+}$  is much larger than both  $\text{Gd}^{3+}$  and  $\text{Ce}^{4+}$  and should facilitate local distortion. One may expect that similar strain-induced effects may be observed in other solids containing oxygen vacancies and two or more ions of different radii in equivalent crystallographic positions. Third, the shift of cations away from an oxygen vacancy may ease the transfer of neighboring oxygen ions into the vacancy. Therefore, our findings provide additional insight into the microscopic origin of the unusually high mobility of oxygen vacancies in pure and doped ceria.

Our findings may also have considerable practical importance for the rapidly developing field of microscopic fuel cells.<sup>[24]</sup> Elastic compatibility of materials can play a critical role in these devices because of the extreme temperature variations which they experience. The fact that dopants similar to Gd in ceria, not only increase ionic conductivity<sup>[25]</sup> but would also be expected to modify elastic properties, may provide a new way to deal with thermally induced stress.

### Acknowledgements

A.K and I.L. acknowledge the Nancy and Stephen Grand Research Center for Sensors and Security and the Israel Ministry of Science for funding this research. This research is made possible in part by the generosity of the Harold Perlman Family. AIF and QW gratefully acknowledge the support of this work by U.S. DOE Grant No. DE-FG02-03ER15476. The use of the NSLS beamlines was supported by U.S. DOE Contract No. DE-AC02-98CH10886. Beamlines X18B and X19A at the NSLS are supported in part by the Synchrotron Catalysis Consortium, U. S. DOE Grant No DE-FG02-05ER15688. Supporting Information is available online from Wiley InterScience or from the author.

Received: June 18, 2009

Revised: October 9, 2009

Published online: January 7, 2010

- [1] I. Riess, R. Koerner, M. Ricken, J. Noelting, *Solid State Ionics* **1988**, 28, 539.  
 [2] H. L. Tuller, *Solid State Ionics* **2000**, 131, 143.  
 [3] A. Atkinson, *Solid State Ionics* **1997**, 95, 249.  
 [4] M. Greenberg, E. Wachtel, I. Lubomirsky, J. Fleig, J. Maier, *Adv. Funct. Mater.* **2006**, 16, 48.  
 [5] A. Kossoy, Y. Feldman, E. Wachtel, I. Lubomirsky, *Adv. Funct. Mater.* **2007**, 17, 2393.

- [6] A. Kossoy, Y. Feldman, R. Korobko, E. Wachtel, I. Lubomirsky, J. Maier, *Adv. Funct. Mater.* **2009**, 19, 634.  
 [7] a) M. Nakayama, M. Martin, *Phys. Chem. Chem. Phys.* **2009**, 11, 3241. b) X. Wei, W. Pan, L. F. Cheng, B. Li, *Solid State Ionics* **2009**, 180, 13.  
 [8] H. Deguchi, H. Yoshida, T. Inagaki, M. Horiuchi, *Solid State Ionics* **2005**, 176, 1817.  
 [9] V. Grover, A. K. Tyagi, *MRS Bull.* **2004**, 39, 859.  
 [10] S. Yamazaki, T. Matsui, T. Sato, Y. Arita, T. Nagasaki, *Solid State Ionics* **2002**, 154, 113.  
 [11] M. Tang, J. A. Valdez, K. E. Sickafus, P. Lu, *Appl. Phys. Lett.* **2007**, 90, 151907.  
 [12] N. Stelzer, J. Nolting, I. Riess, *J. Solid State Chem.* **1995**, 117, 392.  
 [13] E. A. Kummerle, G. Heger, *J. Solid State Chem.* **1999**, 147, 485.  
 [14] J. A. Kilner, *Chem. Lett.* **2008**, 1012.  
 [15] a) P. G. Sundell, M. E. Björketun, G. Wahnström, *Phys. Rev. B* **2006**, 73, 104112. b) E. N. Naumovich, V. V. Kharton, A. A. Yaremchenko, M. V. Patrakeev, D. G. Kellerman, D. I. Logvinovich, V. L. Kozhevnikov, *Phys. Rev. B* **2006**, 74, 064105.  
 [16] H. W. Hayden, W. G. Moffatt, J. Wulff, *The Structure and Properties of Materials*, Vol. 3, Wiley, New York **1965**.  
 [17] J. Philibert, *Atom Movements, Diffusion and Mass Transport in Solids*, Editions de Physique, Les Ulis, France **1991**.  
 [18] H. Inaba, H. Tagawa, *Solid State Ionics* **1996**, 83, 1.  
 [19] H. Lipson, H. Steeple, *Interpretation of X-Ray Powder Diffraction Patterns*, St. Martin's Press, London **1970**.  
 [20] The literature data for the lattice parameter of Gd-doped ceria with Gd concentration less than 40% show exceptionally large variations. The data from eight different sources are compared in Ref. [6]. The same reference presents an experimental proof of the fact that the lattice parameter of  $\text{Ce}_{0.8}\text{Gd}_{0.2}\text{O}_{1.9}$  depends on the sample preparation route and may change with time by a few tenths of a percent.  
 [21] Webelements homepage, www.webelements.com (last accessed Oct. 15, 2009 ).  
 [22] a) J. B. Boyce, J. C. Mikkelsen, *Phys. Rev. B* **1985**, 31, 6903. b) A. Frenkel, E. A. Stern, A. Voronel, M. Qian, M. Newville, *Phys. Rev. B* **1994**, 49, 11662.  
 [23] a) A. Frenkel, E. A. Stern, A. Voronel, M. Qian, M. Newville, *Phys. Rev. Lett.* **1993**, 71, 3485. b) A. Frenkel, A. Voronel, A. Katzir, M. Newville, E. A. Stern, *Phys. B* **1995**, 209, 334.  
 [24] a) L. J. Gauckler, D. Beckel, B. E. Buegler, E. Jud, U. R. Muecke, M. Prestat, J. L. M. Rupp, J. Richter, *Chimia* **2004**, 58, 837. b) A. Evans, A. Bieberle-Hutter, J. L. M. Rupp, L. J. Gauckler, *J. Power Sources* **2009**, 194, 119. c) V. Lawlor, S. Griesser, G. Buchinger, A. G. Olabi, S. Cordiner, D. Meissner, *J. Power Sources* **2009**, 193, 387.  
 [25] H. L. Tuller, *Electrochim. Acta* **2003**, 48, 2879.